"Receptor-based virtual screening and biological characterization of human apurinic/ apyrimidinic endonuclease (Ape1) inhibitors" Ruiz, F.M., Francis, S.M., Tintoré, M., Ferreira, R., Gil-Redondo, R., Morreale, A., Ortiz, A.R., Eritja, R., Fàbrega, C. ChemMedChem, 7(12), 2168-2178 (2012).
doi: 10.1002/cmdc.201200372

Receptor-based virtual screening and biological characterization of new inhibitors of Human Apurinic/Apyrimidinic Endonuclease Enzyme (Ape1)

Federico M. Ruiz[aΨ], Sandrea M. Francis[bΨ], Maria Tintoré[c], Rubén Ferreira[c], Rubén Gil-Redondo[d-e], Antonio Morreale[d*], Ángel R. Ortiz[d], Ramon Eritja [c] and Carmen Fábrega[c]*

[a]*Chemical and Physical Biology, CIB (CSIC;* [b]*Institute of Biomedicine of Valencia, (IBV-CSIC) Valencia;* [c]*Institute for Research in Biomedicine of Barcelona, IQAC-CSIC, CIBER-BBN Networking Centre on Bioengineering Biomaterials and Nanomedicine, Cluster Building, Baldiri i Reixach 10, E-08028 Barcelona E-mail: carme.fabrega@irbbarcelona.org;* [d]*Bioinformatics Unit, CBMSO (CSIC-UAM), Universidad Autónoma de Madrid, Cantoblanco, 28049 Madrid. E-mail: amorreale@cbm.uam.es;* [e]*SmartLigs Bioinformática S.L., Fundación Parque Científico de Madrid, c/ Faraday, 7. Campus de Cantoblanco UAM, E-28049. Madrid, Spain.*

Abstract: The endonucleolytic activity of human apurinic/apyrimidinic endonuclease (AP endo, Ape1) is a major factor in the maintenance of the integrity of the genome. On the other side, as an undesired effect, Ape1 overexpression has been linked to resistance to radio- and chemo-therapy treatments in several human tumors. Inhibition of Ape1 using siRNA or the expression of a dominant-negative form of the protein have been shown to sensitize cells to DNA-damaging agents, including various chemotherapeutic agents. Therefore, inhibition of the enzymatic activity of Ape1 might result in a potent antitumor therapy. Small molecules have been described as Ape1 inhibitors; yet, those compounds are in an early stage of development. Here we report for the first time the identification of new compounds as potential Ape1 inhibitors by using docking-based virtual screening technique. Some of these identified compounds are shown to be active in vitro with activities in the low to the medium micromolar range. Interaction of these compounds with Ape1 protein was observed by mass spectrometry. These molecules also potentiate the cytotoxicity of the chemotherapeutic agent methylmethane sulfonate in fribrosarcoma cells. This study demonstrate the power of the docking and virtual screening techniques as a first step for potential drugs design and opens the door to the development of a new generation of Ape1 inhibitors.

Introduction

Chemo- and radio-therapy are the two main currently available treatments to improve outcomes in cancer patients. The cytotoxicity of many of these agents is directly related to their propensity to induce genomic DNA damage.[1] The persistence of unrepaired DNA damage results in accumulation of mutations, cell cycle arrest and apoptosis.[2] However, the ability of cancer cells to recognize this damage and initiate DNA repair is an important mechanism that impacts negatively upon therapeutic efficacy.[3]

The base excision repair (BER) pathway is the major mechanism for dealing with a variety of lesions in DNA produced by alkylating agents. This pathway is initiated by specific DNA glycosylases, which recognize and excise the damaged base to generate an apurinic/apyrimidinic (AP) site. Ap endonuclease 1 (Ape1) cleaves the phosphodiester backbone adjacent to the 5' side of the AP site, generating a 3' hydroxyl and 5'-deoxy ribose phosphate termini.[4] Polymerase β removes the 5'-deoxy ribose phosphate, fills in the one-nucleotide gap, and the consequent nick is ligated by DNA ligase I or

by DNA ligase III/XRCC1.[5] Ape1 is a fundamental protein in this essential repair pathway and it is thought to be responsible for 95% of total AP endonuclease activity in human cell lines.[6] In addition to its DNA repair activity, Ape1 acts as a redox factor for a variety of important transcription factors such as NF-κappaB, p53, c-Fos and c-Jun.[7] The DNA repair and the redox activities of Ape1 are distinct, both structurally and functionally.

Ape1 protein levels and intracellular distribution have been related to the pathogenesis of several human tumors[5a, 8] and its expression pattern appears to have a prognostic significance in cancer cells, including breast,[8b] lung,[9] ovarian,[8e] gastro-oesophageal[10] and pancreatico-biliary[10] and bone[11] tumors. For this reason, several preclinical and clinical studies have suggested that Ape1 may be an attractive target for anticancer drug development. Using either antisense oligonucleotides or RNA interference approaches, different groups have reported that depletion of intracellular Ape1 sensitizes mammalian cells to a variety of DNA-damaging agents.[5a, 12] In pancreatic cancer cell lines for example, downregulation of Ape1 potentiated the cytotoxicity of gemcitabine.[13] Ape1 downregulation has also been shown to block ovarian cancer cell growth.[14] In melanoma and colon cell lines, Ape1 downregulation led to an increase in apoptosis,[2a, 15] whereas its overexpression conferred protection from cisplatin- or H_2O_2-induced apoptosis.[15] Attempts to create Ape1 knockout mice were embryonically lethal, suggesting that Ape1 is crucial for embryonic development.[16] Heterozygous Ape1 mice were viable but abnormally sensitive to oxidative stress and prone to cancer progression.[17]

Recently, there has been a significant effort towards identifying inhibitors of DNA repair proteins in keeping with the emerging concept that sensitizing cancer tissue to core chemotherapeutic regimens by simultaneous targeting DNA repair may result in enhanced treatment outcomes.[18] As a result of the promising therapeutic potential of the inhibition of Ape1 DNA repair activity, several reports have described the identification and characterization of small molecules that inhibit its repair endonuclease activity,[19] including methoxyamine (MX), lucanthone and 7-nitroindole-2-carboxilic acid (NCA). All three compounds were able to enhance the effects of methylmethane sulfonate (MMS) or temozolamida (TMZ) in ovarian,[20] breast,[20b, 21] colon[22] and HT1080 fibrosarcoma cancer cells.[23] In addition, Lucanthone was able to potentiate the effects of radiation therapy in patients with brain metastasis.[24] However, the evidence of lucanthone topoisomerase inhibitory activity raised a concern regarding an off-target effect[25] and the synergistic cell killing effects observed by NCA with TMZ or MMS were unclear, as recent data showed that its specificity for Ape1 is controversial.[20b, 26] Using a fluorescence-based high-throughput assay, Kelley and co-workers described the identification of 2,4,9-trimethylbenzo[b][1,8]napthyridin-5-amine (AR03), which was found to be active in the low micromolar range *in vitro* against purified Ape1 and inhibited AP site incision activity and its repair in SF67 glioblastoma cells.[27]

Other groups using high-throughput screening (HTS) approaches reported Ape1 inhibitors including compounds containing arylstibonic[28] or bis-carboxilic acid.[29] Reactive Blue 2, 6-hydroxyl-DL-DOPA and myricetin.[30] The bis-carboxilic acid derivatives were not tested in cell based assays,[29] and no information about its *in vivo* activity can be inferred. The arilstibonic acid compounds effectively inhibited Ape1 *in vitro* but were ineffective *in vivo* due to poor cellular uptake.[28] Moreover, antimony-containing compounds are generally considered from a probe development standpoint due to their possible promiscuity akin to the effect of heavy metal ions and their occasional high toxicity.[31] Reactive Blue 2, 6-hydroxyl-DL-DOPA and myricetin were found to have numerous other targets besides Ape1 in cells, therefore they are no such promising agents with selectivity or specificity as Ape1 inhibitors.[30]

We have recently developed a flexible, fully automated virtual screening computational platform (VSDMIP)[32] to identify inhibitors of protein targets from libraries of millions of compounds. This computational platform has been successfully applied to the discovery of new inhibitors of the DNA repair protein O^6-alkylguanine DNA alkyltransferase[33] and in the development of small molecules that compete with ubiquitin E2 variant for its interactions with ubiquitin-conjugating enzyme UBC13, inhibiting its enzymatic activity,[34] among others.

Here we report the identification of novel Ape1 inhibitors by docking-based virtual screening technique. The activity of these compounds has been experimentally proved both *in vitro* and *in vivo*. These

molecules are promising lead candidates to establish quantitative structure-activity relationship models for further development of clinically relevant Ape1 inhibitors as coadjuvants in cancer chemotherapy.

Results and Discussion

Virtual screening (VS)

The virtual screening protocol employed here is summarized in Scheme 1 and briefly described in the Methods section. An essential part of the procedure is to characterize the shape of the active site. For this purpose we used GAGA algorithm (see Methods) to obtain a sort of a negative image of the binding site (Figure 1). Overall, the shape of the active site does not undergo significant conformational changes even after binding to the DNA, as very low RMSD values were obtained after superimposing the different Ape1 structures deposited in the PDB. This fact is reassuring taking into account that the protein flexibility is not explicitly considered during the docking process. The active site is a well-defined deep V-shaped cleft, with a Mg^{2+} cation located in its "elbow".

Upon characterizing the binding site, a library of around 4 million (4,039,777) compounds was first screened using DOCK[35] and the negative image of the binding site. We apply a ZScore (see Methods) cut off value of 4 on the DOCK ranked list, and a set of 2,288 molecules passed onto the next step. These molecules were then re-docked with CDOCK[36] and scored with its molecular mechanics energy function which specifically includes solvent and hydrogen bonding terms. The 100 highest scoring compounds were submitted to MD simulation in explicit solvent and their binding energies estimated and pair-wise decomposed by MM-GBSA[37] calculation over a large collection of snapshots homogenously sampled along the trajectories.

Finally, from the top scoring compounds, and upon visual examination, 15 candidates were selected, were purchased, and tested experimentally. For those showing *in vitro* activity against Ape1, the MM-GBSA[37]method was used to estimate free energy of binding from molecular dynamic trajectories. The physico-chemical properties of the molecules as stored in the ZINC database[38] are shown in Table 1.

Ape1 endonuclease *in vitro* assays

The 15 top-ranked compounds selected from the VS computations where purchased and dissolved in DMSO. The ability of those 15 candidates to inhibit the recombinant Ape1 activity *in vitro* was determined by a fluorescence-based assay described by different groups.[23, 28] In brief, a double stranded DNA (dsDNA) substrate was used containing in one of the strands an internal ribitol (THF) AP site mimic[39] and a 5'6-carboxyfluorescein (FAM) label, while the complementary strand was labeled with a 3'dabcyl fluorescence quencher moiety. The close proximity of the fluorophore and the quencher results in a dampened signal upon light excitation. Following DNA backbone cleavage by Ape1, a short single-stranded DNA fragment 5'-tagged with the FAM group is released from the duplex DNA substrate, resulting in an increase in the fluorescence. Since assay variability is to be expected, we included as a comparative control a compound which was previously described as Ape1 inhibitor (data not shown).[28] Ape1 (at 5.9 nM concentration) was incubated with the dsDNA at 37 ºC for 30 min in the presence of each of the 15 compounds selected during the VS at concentrations of 100 and 200 μM. The results of this first assay showed that compounds **11** to **15** did not exhibit any inhibitory action against Ape1 at these concentrations (Table 1). Compounds **7** to **10** showed an inhibitory effect versus Ape1 at concentration between 150 and 200 μM and were not further evaluated.

On the other hand, compounds **1** to **6** showed inhibitor activity at concentrations below 100 μM and were further analyzed in order to determine the concentration dependence for the inhibition of Ape1 endonuclease activity. All of them inhibited Ape1 with IC_{50} values in the low to medium micromolar range. Compounds **1** and **2** were identified as the most potent inhibitors of Ape1 with an IC_{50} of 2.9 and 5 μM respectively. These two lead compounds had comparative or slightly higher effects in blocking Ape1 activity than thiolactomycin, methyl 3, 4-dephostatin and better than other compounds found by Simeonov and co-workers[30]. Compounds **3** and **4** had an intermediate effect (IC_{50} between 16- 39 μM), whereas compounds **5** and **6** were weakly active showing an IC_{50} >50 μM. This result suggests that

compound **3** and **4** may partially interact with Ape1 through its methoxylphenyl group and that the substitution in *meta* position of the phenyl ring is better tolerated than in *para*. The resultant IC_{50} values obtained for all active compounds are shown in Table 2 and in Figure 2. The chemical structures of these compounds are shown in Figure 3, prioritized by low μM IC_{50} value.

DNA Intercalation binding

To test if these compounds inhibit Ape1 activity via non-specific DNA binding rather than by direct inhibition of the enzymatic activity, we employed a fluorescent dye displacement assay.[30, 40] Briefly, if a compound acts non-specifically by association with DNA, it would displace a DNA-bound fluorophore like Thiazole Orange (ThO) or ethidium bromide. As these molecules emitted fluorescence upon intercalation to DNA, its displacement should produce a decrease in the fluorescence of the complex dye-DNA when increasing amounts of the compounds were added. We selected ThO which binds non covalently to DNA with high affinity instead of ethidium bromide, due to the fact that its fluorescence excitation and emission are red-shifted, which ensures a reduced susceptibility to compound autofluorescence.[30] As shown in Figure 4, compounds **1** to **6** did not displace bound ThO at any range of concentrations starting from 100 pM to 100 μM. This result suggests that these molecules do not inhibit the Ape1 DNA repair activity by a non-competitive effect such as DNA-binding. In contrast, mitoxantrone, described in Simeonov *et al*[30] as a DNA-binding compound, was able to displace ThO producing a 100% decrease in fluorescence in the same concentration range.

Complex formation detected by Mass spectrometry

Electrospray ionization mass spectrometry (ESI-MS) has become an established tool for the investigation of macromolecular complexes.[41] ESI is a gentle ionization method, allowing the analysis of proteins without causing internal fragmentation of the molecule. Their typical multiply charged ions result in low mass-to-charge values which allow an accurate mass determination.[42] The non covalent complex formation of Ape1 with compounds **1** to **6** was analyzed by this means. The mass spectrum of Ape1 alone exhibited a characteristic series of multiply charged positive ions (Figure 5A.a). A narrow range of charge state is a good indication that Ape1 has retained its folded or native conformation. Moreover, the ion mobility measurements further confirmed that the protein was folded during the nano ESI-MS experiments.

The direct observation of the protein-ligand complex ion can be easily achieved for tight binding complexes. However, weakly bound complexes, particularly those dependent on hydrophobic effects, are fragile and may dissociate during desolvation,[43] as we observed with compounds **2**, **3** and **4** (data not shown). The mass spectra of Ape1 in complex with compound **5** (Figure 5A.b) showed that, although any evidence of the complex peaks can be observed, the free protein peaks shifted to a higher mass-to-charge value and this fact may indicate an inhibitor-protein interaction. In the mass spectrum of Ape1 in presence of compounds **1** and **6**, a clear signal of complex formation was observed. Figures 5A.c and 5A.d show the ESI-MS spectra peaks corresponding to free protein (P) and protein in complex with ligand (PL). The complex peaks are zoomed in figure 5B. The estimated stoichiometry of the complex between Ape 1 and the three studied compounds (**1**, **5** and **6)** respectively was equimolar (1:1).

Docking binding modes

For these compounds showing *in vitro* activity against Ape1 the binding mode was estimated by the MM-GBSA[37]method. The binding mode of compound 2 with Ape1 highlights the interaction with the metallic cation, which is the most important energetically. The hydrogen bonding pattern is represented in Figure 7. These interactions were established between: (a) the nitro group of compound 2 and the backbone NH group of residue Asn174; and (b) an oxygen atom from the sulphonyl moiety and the amino group from the side chain of residue Asn212 on the one hand, and the NHε group of residue His309, on the other hand. This binding mode also presented a network of hydrophobic contacts surrounding the quinoxaline core of compound **2** with Phe266, Trp280, and Leu282, and an additional stacking interaction with Tyr269, which stabilizes the benzylpyridinium moiety.

The other 5 active compounds have in common a carboxylic moiety which also presented their main interaction with Ape1 through the Mg^{2+} cation. However, and compared to compound **2**, this interaction is somehow skewed. This fact allows a gradual contribution to the stability of the complex from a salt bridge that is formed between the carboxylic moiety and the side chain of residue Lys98, which in turns depends on the position of the Mg^{2+} cation. Nevertheless, rather similar interaction energies were obtained for the contacts of the ligands with the hydrophobic residues Phe266 and Trp280 and polar Asn174 and Asn212. Finally, an important interaction was established between the central core of the ligands and the side chain of residue Lys98, which is mainly hydrophobic except for compound 1 that forms a hydrogen bond with one of the oxygen atoms in the succinimide-like central moiety.

Effects of cytotoxicity and enhancement of MMS on human cell

The presented data suggested that those 6 compounds can potently and selectively inhibit Ape1 *in vitro*. However, in order to have a general utility as BER inhibitors, it is important to confirm that they can block Ape1 function in living cells. The colony forming assay was used in order to study the capability of compounds **1** to **6** to enhance MMS cytotoxicity in HOS cells.[11, 20b, 21, 23, 44] MMS creates base damage by methylation, which is either lost spontaneously or excised by the alkylpurine DNA glycolsylase, resulting in a high number of cytotoxic abasic sites.[45] Inhibition of Ape1 in cell culture or the expression of a dominant negative form of the protein has been shown to increase sensitivity of human cells to MMS.[11, 20b, 21, 23, 44]

Cells were incubated with the 6 compounds before, during and after MMS treatment to ensure that inhibitors were present during the entire period of time needed for DNA damage to be formed. We analyzed the colony formation efficiency of HOS cells exposed to MMS alone, each inhibitor alone, or the combination of MMS plus inhibitor, compared to a non-exposed control. MMS alone reduced the number of colonies by 15% and, as shown in Figure 7, all six compounds enhance MMS cytotoxicity. Compounds **1** and **3** are less effective sensitizing tumoral cell to MMS than the rest, requiring a concentration up to 100 μM in order to obtain a 50% increase in cell killing. This lower sensitizing effect of compound **3** is consistent with its slightly smaller *in vitro* affinity for Ape1. However, the inefficiency of compound **1** was unexpected on the basis of its high ability to inhibit Ape1 activity *in vitro*. This observation suggested that it may not be able to cross cell membranes or it could be degraded before reaching its final target. Compound **4** had almost no effect on the cytotoxicity produced by MMS, only a little decrease in cell survival was observed at 50 μM, which was not incremented when cells were incubated with higher concentrations of this compound. Compound **5** exhibited an increasing capability to enhance the killing effect of MMS with an EC_{50} value around 50 μM, which is close to the IC_{50} value obtained in the *in vitro* experiments. Compound **6** showed a promising lethality (around 50 μM), even if at higher concentrations it was unable to increase the effect of MMS in the cells.

The combination of MMS and compound **2** presented the best result *in vivo*. Its lethality was found to be in the lower micromolar range (7.5 μM), being consistent with its affinity for Ape1 *in vitro*. The results observed for this lead compound opens the door for their further optimization as Ape1 inhibitors.

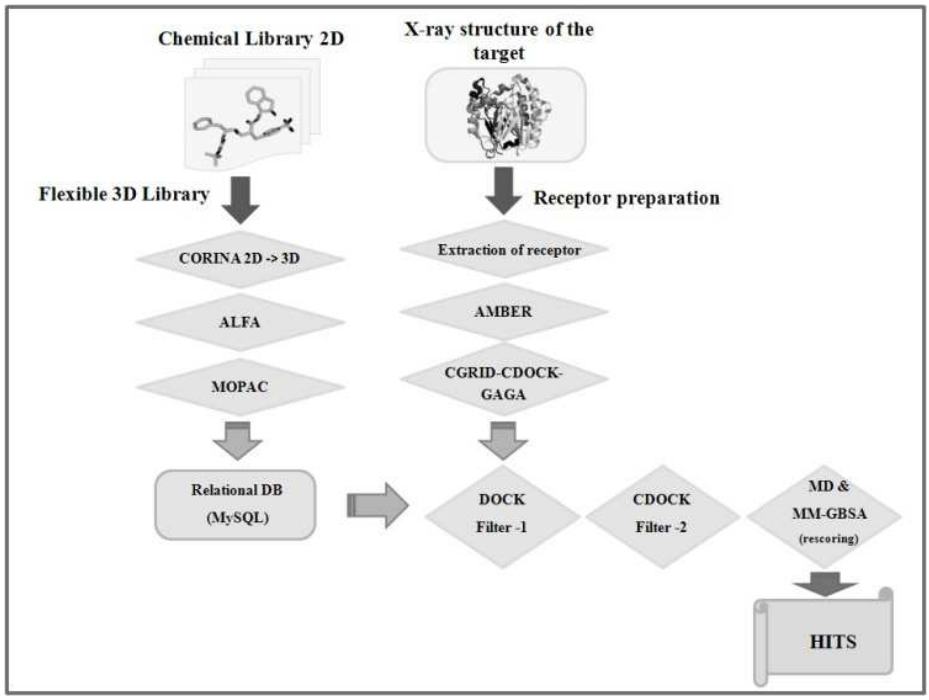

Scheme 1. Flowchart of the virtual screening procedure applied in this work.

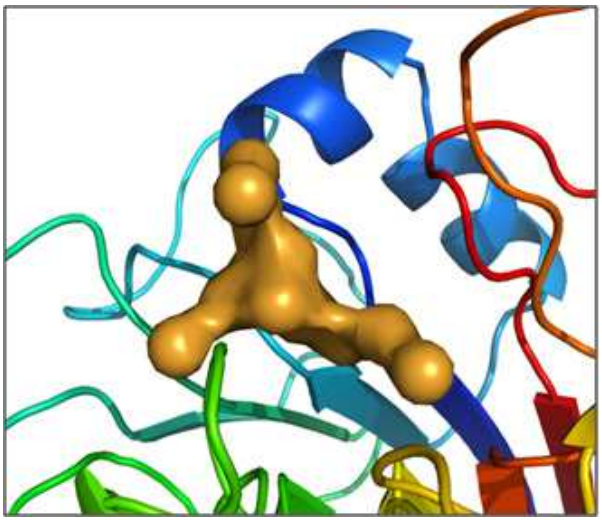

Figure 1. Inside view of the active site of Ape1 with the ligand negative spheres image computed with GAGA.

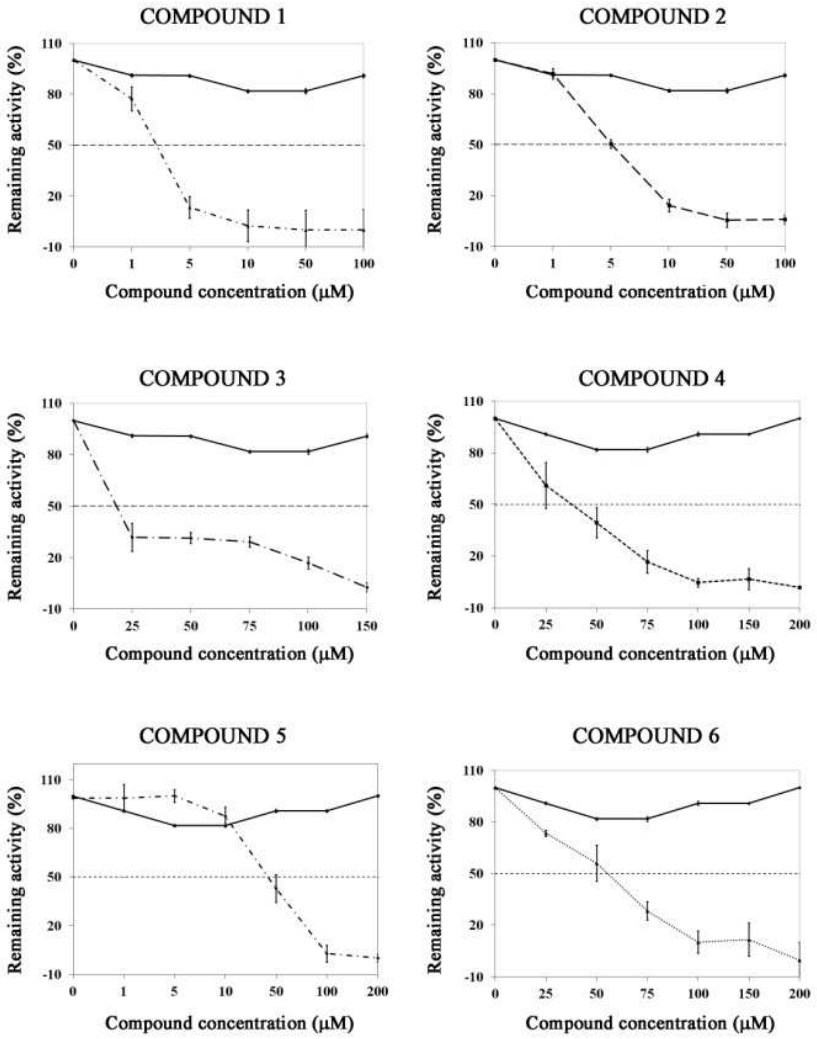

Figure 2. Concentration curve showing the inactivation of human apurinic/apirimidinic endonuclease Ape1 by compounds **1** to **6**. Remaining Ape1 activity vs. compound concentration was plotted, relative to untreated control samples. The effect of the compound solvent (DMSO) on Ape1 activity is showed in a continuous line. Dotted line marks 50% remaining Ape1 activity. Compounds 1 to 3 show inhibitory effect on Ape1 activity in the lower micro molar range. Compounds 4 to 6 show inhibitory effect on Ape1 activity in the medium micro molar range. Each graph represents the average of triplicates of three separate experiments.

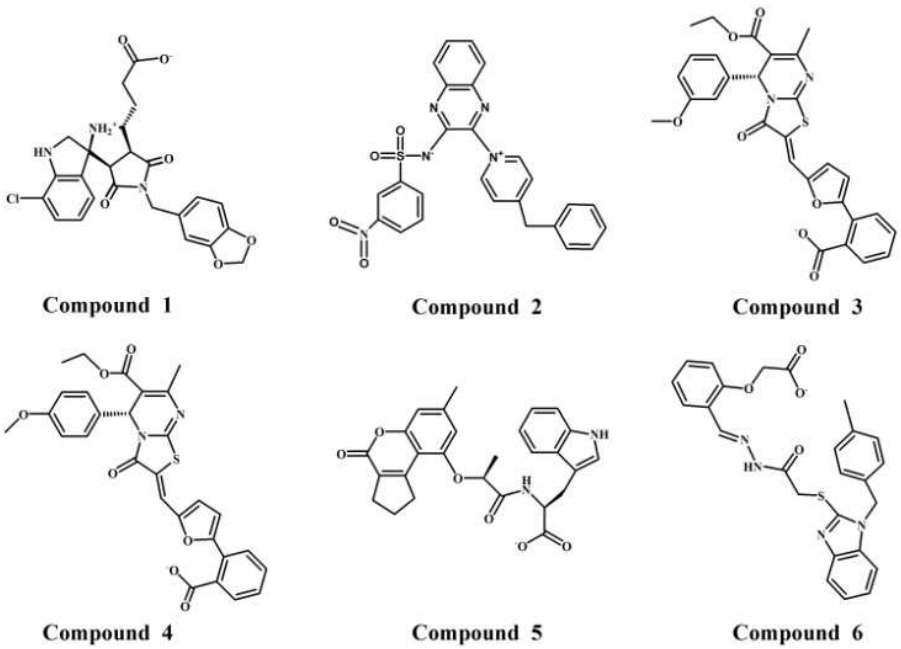

Figure 3. Chemical structures of the six compounds that showed Ape1 inhibition in the micro molar range.

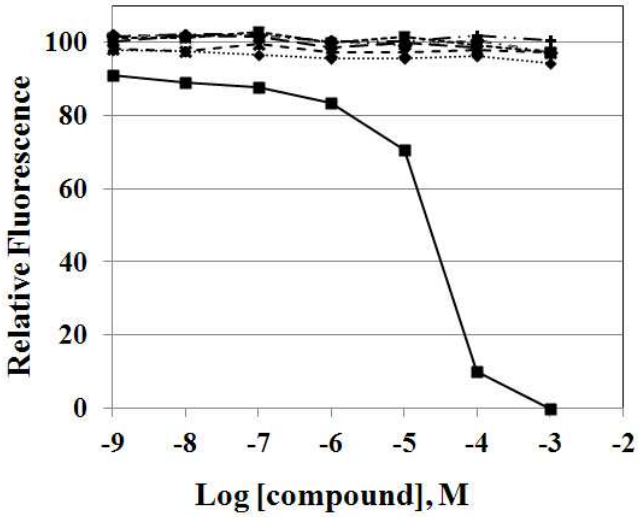

Figure 4. ThO inhibitor displacement assays. A ThO competition assay was used to evaluate the ability to bind DNA of all the Ape1 compounds which were active in the *in vitro* assay (**1, 2, 3, 4, 5** and **6**). No decrease in ThO fluorescence was observed upon the addition of the compounds, indicating that these compounds do not bind DNA. Mitoxantrone a clear DNA-binding molecule was used as positive control (filled squares). Fluorescence signal was normalized against DNA.

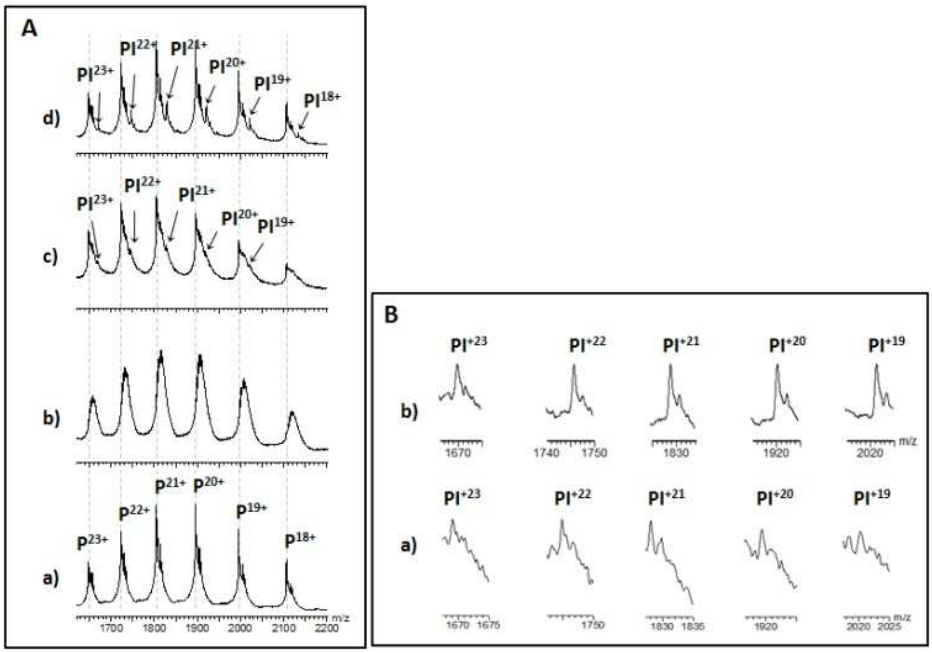

Figure 5. Complex formation identified by Mass spectrometry. Ape1 (28 µM) was mixed with each inhibitor (140 µM) on 100 mM ammonium acetate buffer and let to equilibrate at 4ºC for one hour as described in Materials and Methods. A) ESI-MS spectra of a) Ape1 b) Ape1 with compound **5** c) Ape1 with compound **6** and d) Ape1 with compound **1**. B) Zoom of the complex regions: a) Ape1 with compound **6** and b) Ape1 with compound **1**.

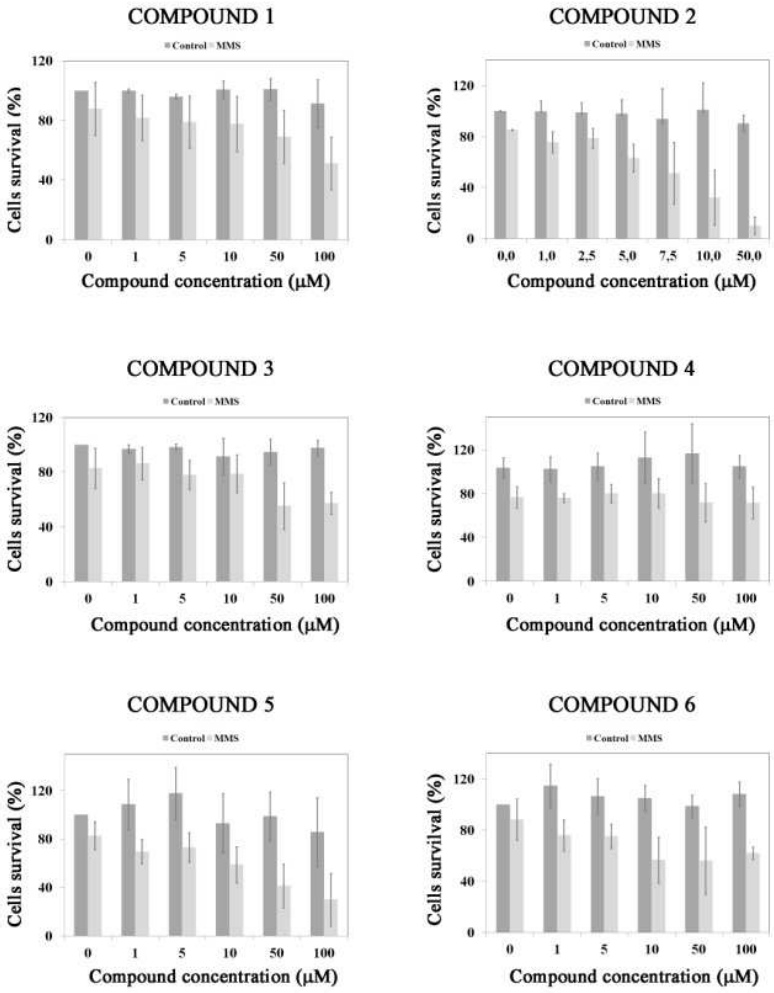

Figure 6. Effect of compounds 1 to 6 in HOS cells survival, relative to untreated cells. Light grey bars show samples with no MMS added in the presence of different concentrations of each of the 6 compounds, dark grey bars show the same experiment in the presence of MMS at 300 µM. MMS alone reduced the cell number to an average of 15%. Each graphic represents the average of duplicates of three separate experiments.

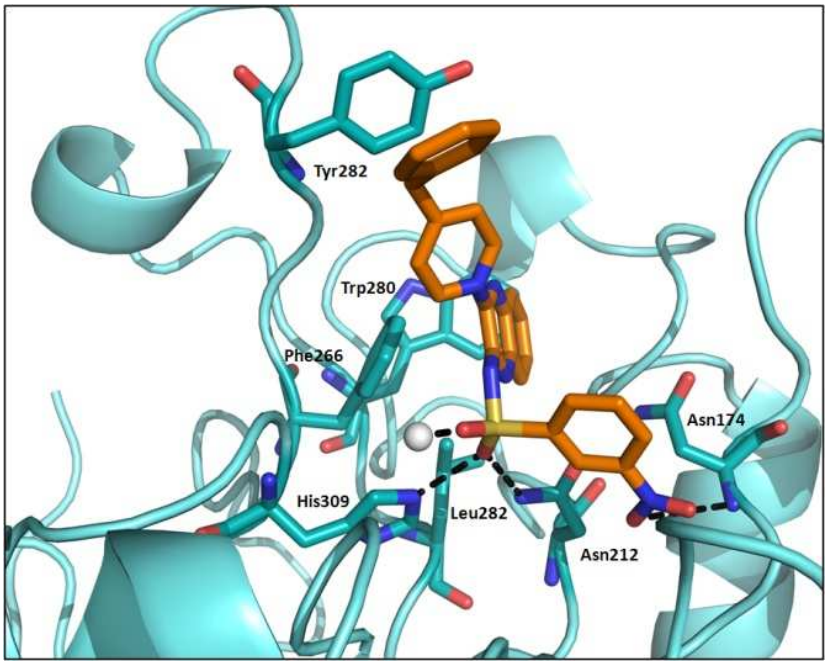

Figure 7. Average minimized structure of the compound 2-Ape1 complex after the molecular dynamics simulations. The color code is as follows: the protein is represented as cartoons in cyan. The side chains of main interacting residues are colored by atom type: C in cyan, N in blue, and O in red. In compound 2, C atoms are in orange, N in blue, O in red and the S atom in yellow. Hydrogen atoms are omitted for clarity. The gray sphere represents the Mg^{2+}. Dashed lines correspond to the hydrogen bond interactions.

Table 1. List of the 15 top-ranked compounds obtained in the virtual screening . The computed chemical properties (as found in the ZINC database and the *in vitro* and *in vivo* activities of the active compounds are shown. [a]MW molecular weight; [b]Average interaction energy during the MD simulation in kcal/mol; [c]*in vitro* IC_{50} value (concentration of compound required to produce a 50% reduction in Ape1 activity). [d]*in vivo* EC_{50} value (concentration of compound required to produce a 50% of cell killing in the presence of 300 μM MMS). [f]ND not determined. *The IC_{50} and the EC_{50} values represented the average of three separate experiments.

	ZINC id	Log P	H-bond donors	H-bond acceptors	Charge	MW	IC_{50} (μM)[c*]	EC_{50} (μM)[d*]
1	ZINC08790444	1,57	3	10	0	497,89	2,9 ± 0,55	>100
2	ZINC09086704	1,82	0	9	0	497,54	5 ± 0,55	7,5
3	ZINC00708759	6,37	0	9	-1	543,58	16,96 ± 0,64	>50
4	ZINC00870176	6,39	0	9	-1	543,58	38,5 ± 0,80	>100
5	ZINC00730105	4,79	1	8	-1	487,56	51,76 ± 0,86	(10-50)
6	ZINC02118845	1,97	2	8	-1	473,51	55,55 ± 0,80	50
7	ZINC04059809	5,19	0	8	-1	427,48	> 130	ND
8	ZINC08854784	2,61	0	12	0	477,50	>150	ND
9	ZINC08877288	2,12	3	9	-1	493,58	> 150	ND
10	ZINC04060698	4,63	0	8	-1	413,45	> 150	ND
11	ZINC03583501	3,69	0	9	0	523,95	> 200	ND
12	ZINC08932744	3,48	2	6	0	440,52	> 200	ND
13	ZINC09042551	1,91	3	9	-1	423,45	> 200	ND
14	ZINC04202254	3,97	0	8	-1	456,53	> 200	ND
15	ZINC00706278	2,61	0	8	-1	421,41	> 200	ND

Table 2. Interaction energy analysis as computed from the molecular dynamics simulations by the MMGBSA approach, for the six active molecules found in this work. All values are in kcal/mol.

	Compounds					
Residue	1	2	3	4	5	6
Lys98	-1.75	-0.3	-5.97	-1.93	-4.85	-1.94
Tyr128	-0.23	-0.13	-0.16	-0.87	-1.99	-0.53
Asn174	-0.3	-2.45	-2.56	-1.98	-3.23	-0.34
Arg177	-3.91	-0.3	-2.81	-7.47	-4.25	-5.42
Asn212	-0.34	-6.27	-1.85	-0.17	-1.49	-0.23
Phe266	-1.94	-3.04	-3.55	-1.51	-2.94	-1.09
Thr268	-1.2	-0.56	-1.92	-2.51	-1.38	-0.84
Tyr269	-3.38	-3.31	-0.38	-1.44	-0.03	-1.22
Trp280	-2.1	-1.31	-2.2	-1.43	-3.65	-0.04
Leu282	-0.68	-1.4	-1.02	-0.14	-0.78	-0.09
Asp308	-0.04	6.07	2.33	0.54	0.08	-3.46
His309	-0.31	-7.83	-0.66	-0.42	-0.47	-0.5
Mg^{2+}	-59.51	-37.66	-41.01	-56.41	-60.33	-70.59

Conclusion

Several classes of inhibitors of Ape1 have been described previously. However, the specificity of some of these compounds for Ape1 remain unclear[25] or a bit controversial.[20b, 26] Here, we have applied docking-based virtual screening technique to select as hit compounds a concrete number of molecules (15 compounds) from a 4 million library, to become novel and more potent Ape1 inhibitors. Six of these molecules selected from the ZINC database were found to be active. In particular, two of them are single-digit micromolar inhibitors against purified Ape1 (similar or even more potent than prior reported inhibitors), with the capacity to potentiate the cytotoxity of a relevant DNA-damaging agent like MMS. The predicted binding modes highlighted the interaction with the metallic cation, which is the most important energetically, the hydrogen bonding with residues Asn174 and Asn212, and a network of hydrophobic contacts of the ligands with the Phe266 and Trp280. In the case of compound **2**, the most important interactions with Ape1 are mainly established through the quinoxaline core.

In summary, novel compounds have been identified as potent leads of Ape1 DNA repair inhibition. The binding properties, cellular uptake and solubility of these compounds can be further optimized to produce a subfamily of candidates with improved pharmacological properties. This new generation of compounds could lead to innovative drugs that may act as coadjuvants in cancer chemotherapy.

Experimental Section

Materials.

The Ape1 gene (Homo sapiens) inserted into the pOTB7 vector was obtained from the Genomics Unit (Clone id: IMAGE 2823545) at the Centro Nacional de Investigaciones Oncologicas (CNIO). The pet28a plasmid and the competent *Escherichia coli* strains (DH5α, BL21(DE3), Rosetta) were purchased from Novagen. The enzymes and their corresponding buffers for cloning were purchased from Fermentas or New England Biolabs. The chemical reagents used for the expression and purification steps were purchased from Sigma, Merck, Bio-Rad or Fluka, and the SDS-PAGE standards, gels and buffers, from Invitrogen. HiTrap FF and size exclusion (HiLoad Superdex 75 16/60) columns were purchased from GE Healthcare.

The oligonucleotides 5'-FAM-GAGAA[X]ATAGTCGCG-3' and 3′-Q-CTCTTGTATCAGCGC-5′ (where FAM is Fluorescein, Q is Dabsyl and X is ribitol,[46] an abasic site analog (AP)) site were custom-made by Sigma. Candidate compounds were purchased from different companies, in particular compounds **1, 5** and **6** were obtained from IBScreen; **2** was obtained from Enamine and compounds **3, 4** were obtained from Specs. Stock solutions were prepared by dissolving them in DMSO at a final concentration of 1 mM and kept at -20 $^{\circ}$C until further use. The fluorescence assay was carried out on a spectrofluorometer Multi-Detection microplate reader Biotek FLx800 and a Jasco FP6200, in optical 96-well reaction plates.

Human osteosarcoma cells, (ATCC Number HOS) were cultured in RPMI 1640 medium (Gibco) supplemented with 10% fetal bovine serum (Invitrogen). Methylmethanosulfonate (MMS) was obtained from Sigma.

Virtual Screening (VS). All VS calculations were performed within the automated platform VSDMIP[32] (Virtual Screening Data Management on an Integrated Platform), see Figure 1. For clarity, we briefly describe here the main steps comprising the protocol (Scheme 1).

Receptor preparation. The crystal structure of 1HD7 (PDB ID code)[47] was selected as a receptor since no substantial differences were found in the active site amongst the available Ape1 structures and it presented the highest resolution structure (1.95 Å). All atoms other than the receptor were deleted except for the divalent metal (Pb^{2+}) in the active site, which in order to resemble *in vivo* conditions, was replaced by magnesium, the preferred metal cofactor of the human Ape1 enzyme.[48] AMBER8 ff99[49] force field was then used to assign atom types and charges for each atom in the receptor. Hydrogen atoms were added assuming standard protonation states of titratable groups, except for the key interacting residues, in which the hydrogen atoms were assigned based on the information given from the H++ web server.[50]

For this purpose, the receptor was submitted to the server and a Generalized Born model was used for the pKa calculation at pH=6.5 with 0.15 M salt concentration and an internal and external dielectric constant of 4 and 80, respectively. The histidine residue His309, present in the binding site, was found to be protonated, which is consistent with an NMR study done by Lowry *et al.*[51]

Binding site definition and characterization. To delimit the binding site PDB codes 1HD7[47] (Ape1 apo form) and 1DEW[52] (Ape1 bound to DNA, subunit A) were superimposed, (RMSD among Cα carbon atoms ~0.28 Å) selecting a DNA fragment as the core around which to build the docking box by adding a 5.0 Å *cushion* to its maximum dimensions. This DNA fragment consists of an abasic sugar connected to a cytosine nucleotide residue to its 5' end and including the following 5' phosphate. An equally spaced grid of 0.375 Å was then built, and CGRID[36] was used to calculate receptor interaction fields, a 12-6 Lennard-Jones term. The electrostatic term was modeled with a sigmoidal dielectric screening function using typical atom probes (C, H, N, O, S, P, F, Cl, Br, and I) at each grid point. Next benzene, water and methanol probes were docked with CDOCK[36] to generate intermolecular interaction energy maps aimed to capture the most favorable hydrophobic, hydrophilic and hydrogen bonds interaction areas, respectively. These areas were further compressed into Gaussian functions using GAGA algorithm,[53] producing a sort of negative image of the interaction site. The putative active ligands in the library must conform to this approximate shape.

Chemical library preparation. Ligands for VS consisted of a library with more than 4 million (4,039,777) non-redundant molecules, obtained from the publicly available ZINC database[38] in SMILES format.[54] Multiple protonation states and tautomeric forms were considered as implemented by default in ZINC database.[39] The molecules were then processed within VSDMIP[32] as follows: a) conversion from SMILE to 3D MOL2 using CORINA,[55] b) atomic charges calculations with MOPAC[56] (MNDO ESP method) on every single structure provided by CORINA, and c) atom types assignment according to the AMBER ff99[49] force field and conformational analysis with ALFA.[57]

Filter 1**.** An initial filter was performed with the docking program DOCK[35] to quickly discard those molecules that do not geometrically fit within the binding site. The spheres needed by DOCK were generated previously with GAGA. We used DOCK contact as scoring function, normalizing the score values ($score_i$) by converted them into ZScore using mean (average score) and standard deviation (σ) values ($ZScore_i = (score_i\text{-average score})/\sigma$). Only molecules with a ZScore beyond a cut off value of 4 were selected and 2,500 passed onto the next step.

Filter 2. Selected molecules from filter 1 were studied with the more accurate docking algorithm CDOCK.[36] CDOCK exhaustively docks each molecule within the binding site of the receptor using the interaction energy grids previously calculated with CGRID. This was achieved by an exhaustive exploration of the location and orientation of each molecule by positioning its centers of mass on grid points, where discrete rotations of 27º arc on each axe are performed. Finally, the energy for each pose was evaluated by the molecular mechanism force-field scoring function implemented in CDOCK, which besides including a 12–6 Lennard-Jones term and an electrostatic term modeled with a sigmoidal dielectric screening function, also accounts for ligand and receptor desolvations as well as for hydrogen bonding interactions.[58]

Molecular dynamics simulations. The top ranked 100 molecules according to CDOCK's scoring function were subjected to a more exhaustive binding free energy estimation by a combination of molecular dynamics (MD) trajectories and MM-GBSA[37] calculation on these trajectories. The 100 complexes were hydrated by using boxes containing explicit water molecules, energy minimized, heated (20 ps), and equilibrated (100 ps). Then when the equilibration was reached, MD trajectories were continued for 2 ns. Structures were homogenously sampled at each ps and stored for post-processing. All the simulations were performed at constant pressure and temperature (1 atm and 300 K) with an integration time step of 2 fs. SHAKE[59] was used to constrain all the bonds involving H atoms at their equilibrium distances. Periodic boundary conditions and the Particle Mesh Ewald methods were applied to treat long-range electrostatic effects.[60] AMBER ff99[49] and TIP3P[61] force-fields were used in all cases. Finally, the effective binding free energies were qualitatively estimated with the MM-GBSA[37] approach, which calculates the free energy of binding as a sum of a Molecular Mechanics (MM) interaction term, a solvation contribution thorough a Generalized Born (GB) model and a Surface Area (SA) contribution to account for the non-polar part of desolvation. A 12–6 Lennard-Jones term was used

to model de MM contribution. For GB, the solute dielectric constant was set to 4 while that of the solvent was set to 80, and the dielectric boundary was calculated using a solvent probe radius of 1.4 Å. The SA contribution was approximated as a linear relationship to the change in SASA (Solvent Accessible Surface Area):

$\Delta G_{np} = a + b\,\Delta SASA$

where *a* is 0.092 kcal·mol^{-1}, *b* is 0.00542 kcal·mol^{-1}Å^{-2}, ΔG_{np} is the SA contribution, and the change in SASA refers to the complex SASA minus the sum of that of the receptor and the ligand alone. In addition, interaction energy analysis between the ligands and the more relevant residues in the binding site were computed (with MM-GBSA) and are contained in Table 2. All the trajectories and analysis were performed using the AMBER 8 computer program and associated modules.[62]

Selection of candidates. Among the 100 molecules with highest scoring values 15 were selected upon visual examination. All visualizations were done within the molecular graphics program PyMOL.[63] Averaged structures along the MD trajectories were obtained and minimized in vacuum with the ff99 force field, without periodic boundary conditions and during 1000 steps (the first 500 with the steepest descent method and the rest with the conjugated gradient) solely to alleviate the possible clashes that may be originated by averaging the coordinates. These structures were used for graphical representation and comparison of the binding modes. Finally, those 15 selected compounds were purchased and tested experimentally.

Inhibition of Ape1 Activity

Protein Production and Purification. The *in vitro* assays were carried out using recombinant Ape1. The cDNA of full length Ape1 (IMAGE:2823545) was amplified by PCR using primers 5'-CCCGGG**CATATG**CCGAAGCGTGGGAAAAAG-3'and 5'GCC**CTCGAG**TCACAGTGCTAGGTATAGG-GT-3', that incorporated the NdeI and XhoI restriction enzymes sites respectively. The PCR product was cloned into the pet-28a(+) (Novagen) vector. The resulting construct, Ape1-pet28a, was verified by nucleic acid sequencing. The protein was expressed in the *E. coli* strain BL21 and once the culture reached an OD_{600} value of 0.6 it was induced by adding 1 mM IPTG during 3 h at 30 ℃. The pellet from a 2 L culture was disrupted by sonication and centrifuged. The supernatant was filtered, loaded into a HiTrap^{TM} FF column (GE Healthcare), and eluted with an Imidazole gradient. Finally, the protein was loaded into a Superdex 75 16/60 column (GE Healthcare), being the buffer 300 mM NaCl, 20 mM Tris pH 8.0, 1 mM DTT and 5% v/v glycerol.

Ape1 Activity Assay. The *in vitro* AP site cleavage assay was carried out using a modified version of the protocol that had been described previously.[23, 28] Briefly, Ape1 enzyme (5,9 nM) was incubated with or without compounds (at 100 and 200 μM) in a buffer containing 50 mM Tris–HCl (pH 8.0), 1 mM $MgCl_2$, 5 mM NaCl and 2 mM dithiothreitol (DTT) at room temperature for 30 min. The sequence 5'-FAM-GAGAA[X]ATAGTCGCG-3' and its complementary oligonucleotide 3′-Q-CTCTTGTATCAGCGC-5′ were annealed to form a double stranded DNA and the reaction was initiated by addition of the annealed substrate. Fluorescence readings were taken continuously after 30 min incubation at 20℃, at excitatio n and emission wavelength of 485 and 535 nm, respectively. Hits from the initial screen were analyzed further for inhibitory potency using decreasing dilutions of inhibitor. Each compound concentration was assayed in triplicate and experiments repeated three times. Percent inhibition was calculated relative to untreated DMSO-control samples. Bovine serum albumin (BSA) was used as a negative control (data not shown). The IC_{50} values were determined graphically from plots of remaining activity vs. inhibitor concentration.

DNA Intercalation Assay. A modified version of the ethidium bromide-based DNA binding assay was carried out essentially as described previously.[30, 40] In brief, a mixture of 500 nM of unlabeled double stranded DNA and 2.5 μM ThO in Ape1 reaction buffer in 400 ul total volume was prepared. Compounds (at concentrations in the range of 100 pM to 100 μM) were added, and the fluorescence signal (excitation 501 nm and emission 530 nm) was measured after 10 minutes of incubation at room temperature in 50 mM Tris-HCl, pH 7.5, 50 mM NaCl, 10 mM MgCl2 and 1 mM EDTA. Each compound concentration was assayed in triplicates. Percentage fluorescence was calculated relative to the total fluorescence acquired with double stranded DNA and 2.5 μM ThO.

Mass analysis of the non-covalent complex between Ape1 and lead compounds. Mass spectrometry experiments were performed on Waters (Manchester, UK) instrument equipped with electrospray ionisation, a travelling wave ion mobility cell and a time-of-flight mass analyser. Synapt G1 was interfaced to a chip-based nanoESI device, (Advion, Triversa Nanomate). This device contains a 96 -well sample plate, 96 disposable spraying tips and an ESI chip with 100 nozzles in front of the inlet of the mass spectrometer. The instrument was operated in the automatic mode using a contact closure signal. A spraying voltage of +1.76 kV and a sample pressure of 5.80 psi were applied. Each well was loaded with 10µl of sample, from which a total of 4 µl was infused during 10 min. Operating conditions for the Synap G1 mass spectrometer were: cone voltage = 20V; extraction cone = 5.5 V; source temperature = 20 ºC; trap and transfer voltages = 6 V and 4V, respectively. The ion mobility cell was filled with N_2 and an electric field was applied to the cell in the form of waves (wave height = 9.5 V) that passed thought the cell at 300 m/s. The bias voltage for ion introduction into the IMS cell was 15V.

The Ape1 buffer was exchanged to 100 mM ammonium acetate pH=7 to prevent buffer interferences in the mass spectrometry experiments. Once we confirmed the mass spectrum for the native form of Ape1, we proceeded to analyze the non-covalent inhibitor-protein complexes. Ape1 (28 µM) was mixed with (140 µM of) each inhibitor (**1** to **6**) separately and let to equilibrate at 4ºC for one hour. Ape1 in the presence of DMSO or an inactive molecule (**16**) were used as Mass spectrum controls.

Cell culture cytotoxic assay. The effect of compounds **1** to **6** on the sensitivity of human osteosarcoma cells (HOS) to methyl methanesulfonate (MMS) was determined using colony formation assays as it has been previously described in Ape1 inhibition studies[28]. HOS cells were seeded at 10 x 10^3 cells per well density in 24-well, flat-bottomed plates and incubated in a humidified, 5% CO_2 incubator at 37^{o}C for 36 h. Compound solutions were diluted in the culture medium at final concentrations of 100, 50, 30, 20, 5, 2.5 and 1 µM, and were immediately used to treat the cells. Cells were incubated with these compounds' solutions for 6 h and then MMS (or the equivalent volume of the vehicle as negative controls) was added to a final concentration of 300 µM. After 2 h of incubation, the medium was replaced with fresh medium containing the same compound concentration, and cells were left to grow for an additional 16 h. The cells were then replated at densities of 2000 cells per well in 24-well plates and grown for 1 week until discrete colonies were formed. Colonies were washed twice with PBS and stained with a 0.5% crystal violet - 20% ethanol solution. Cells were rinsed with deionized water and air dried. Stained colonies were counted in a ELx 800 Universal Microplate Reader (Bio-Tek Instruments INC) and clonogenic survival was determined relative to untreated cells. Samples were assayed in duplicates and experiments repeated three times.

Acknowledgements

This work was supported by "Fondo de Investigaciones Sanitarias" (grant PI06/1250), by "Ministerio Ciencia e Innovación" (grant CTQ-2010-20541-C03-03), by "Comunidad de Madrid" (SBIO-0214-2006 [BIPEDD] and S2010-BMD-2457 [BIPEDD2]). C.F is greateful to Generalitat de Catalunya and Instituto de Salud Carlos III for a SNS Miguel Servet contract. R.G.-R. enjoyed a MICINN contract from "Programa de Personal Técnico y de Apoyo 2008". F.M.R was supported by a Junta de Ampliación de Estudios-Doc contract. A.M. acknowledges financial support from Fundación Severo Ochoa through the AMAROUTO program. Generous allocation of computer time at the Barcelona Supercomputer Center is gratefully acknowledged. Finally, this work is dedicated to the memory of Ángel Ramírez Ortiz who has been a great mentor, colleague, and friend.

Keywords: DNA repair, Chemotherapy, inhobitors of apurinic/apyrimidinic endonuclease (Ape 1), Structure-based drug design (SBDD), drugs.

REFERENCES

[1] a)M. Christmann, M. T. Tomicic, W. P. Roos, B. Kaina, *Toxicology* **2003**, *193*, 3; b)O. Fleck, O. Nielsen, *J Cell Sci* **2004**, *117*, 515; c)T. Lindahl, *Nature* **1993**, *362*, 709.

[2] a)H. Fung, B. Demple, *Mol Cell* **2005**, *17*, 463; b)L. A. Loeb, B. D. Preston, *Annu Rev Genet* **1986**, *20*, 201.
[3] D. B. Longley, P. G. Johnston, *J Pathol* **2005**, *205*, 275.
[4] D. M. Wilson, 3rd, M. Takeshita, A. P. Grollman, B. Demple, *J Biol Chem* **1995**, *270*, 16002.
[5] a)A. R. Evans, M. Limp-Foster, M. R. Kelley, *Mutat Res* **2000**, *461*, 83; b)A. B. Robertson, A. Klungland, T. Rognes, I. Leiros, *Cell Mol Life Sci* **2009**, *66*, 981.
[6] a)B. Demple, T. Herman, D. S. Chen, *Proc Natl Acad Sci U S A* **1991**, *88*, 11450; b)D. S. Chen, T. Herman, B. Demple, *Nucleic Acids Res* **1991**, *19*, 5907; c)J. H. Hoeijmakers, *Nature* **2001**, *411*, 366.
[7] a)S. Xanthoudakis, G. Miao, F. Wang, Y. C. Pan, T. Curran, *EMBO J* **1992**, *11*, 3323; b)T. Okazaki, U. Chung, T. Nishishita, S. Ebisu, S. Usuda, S. Mishiro, S. Xanthoudakis, T. Igarashi, E. Ogata, *J Biol Chem* **1994**, *269*, 27855; c)K. K. Bhakat, T. Izumi, S. H. Yang, T. K. Hazra, S. Mitra, *EMBO J* **2003**, *22*, 6299; d)L. J. Walker, C. N. Robson, E. Black, D. Gillespie, I. D. Hickson, *Mol Cell Biol* **1993**, *13*, 5370.
[8] a)M. S. Bobola, A. Blank, M. S. Berger, B. A. Stevens, J. R. Silber, *Clin Cancer Res* **2001**, *7*, 3510; b)S. Kakolyris, L. Kaklamanis, K. Engels, S. B. Fox, M. Taylor, I. D. Hickson, K. C. Gatter, A. L. Harris, *Br J Cancer* **1998**, *77*, 1169; c)Y. Xu, D. H. Moore, J. Broshears, L. Liu, T. M. Wilson, M. R. Kelley, *Anticancer Res* **1997**, *17*, 3713; d)C. J. Herring, C. M. West, D. P. Wilks, S. E. Davidson, R. D. Hunter, P. Berry, G. Forster, J. MacKinnon, J. A. Rafferty, R. H. Elder, J. H. Hendry, G. P. Margison, *Br J Cancer* **1998**, *78*, 1128; e)D. H. Moore, H. Michael, R. Tritt, S. H. Parsons, M. R. Kelley, *Clin Cancer Res* **2000**, *6*, 602; f)B. Thomson, R. Tritt, M. Davis, M. R. Kelley, *J Pediatr Hematol Oncol* **2001**, *23*, 234; g)M. I. Koukourakis, A. Giatromanolaki, S. Kakolyris, E. Sivridis, V. Georgoulias, G. Funtzilas, I. D. Hickson, K. C. Gatter, A. L. Harris, *Int J Radiat Oncol Biol Phys* **2001**, *50*, 27; h)G. Fritz, S. Grosch, M. Tomicic, B. Kaina, *Toxicology* **2003**, *193*, 67.
[9] a)S. Kakolyris, A. Giatromanolaki, M. Koukourakis, L. Kaklamanis, P. Kanavaros, I. D. Hickson, G. Barzilay, V. Georgoulias, K. C. Gatter, A. L. Harris, *J Pathol* **1999**, *189*, 351; b)F. Puglisi, G. Aprile, A. M. Minisini, F. Barbone, P. Cataldi, G. Tell, M. R. Kelley, G. Damante, C. A. Beltrami, C. Di Loreto, *Anticancer Res* **2001**, *21*, 4041.
[10] A. Al-Attar, L. Gossage, K. R. Fareed, M. Shehata, M. Mohammed, A. M. Zaitoun, I. Soomro, D. N. Lobo, R. Abbotts, S. Chan, S. Madhusudan, *Br J Cancer* **2010**, *102*, 704.
[11] D. Wang, M. Luo, M. R. Kelley, *Mol Cancer Ther* **2004**, *3*, 679.
[12] a)L. J. Walker, R. B. Craig, A. L. Harris, I. D. Hickson, *Nucleic Acids Res* **1994**, *22*, 4884; b)Y. Ono, T. Furuta, T. Ohmoto, K. Akiyama, S. Seki, *Mutat Res* **1994**, *315*, 55; c)D. S. Chen, Z. L. Olkowski, *Ann N Y Acad Sci* **1994**, *726*, 306; d)J. R. Silber, M. S. Bobola, A. Blank, K. D. Schoeler, P. D. Haroldson, M. B. Huynh, D. D. Kolstoe, *Clin Cancer Res* **2002**, *8*, 3008.
[13] J. P. Lau, K. L. Weatherdon, V. Skalski, D. W. Hedley, *Br J Cancer* **2004**, *91*, 1166.
[14] M. L. Fishel, Y. He, A. M. Reed, H. Chin-Sinex, G. D. Hutchins, M. S. Mendonca, M. R. Kelley, *DNA Repair (Amst)* **2008**, *7*, 177.
[15] S. Yang, K. Irani, S. E. Heffron, F. Jurnak, F. L. Meyskens, Jr., *Mol Cancer Ther* **2005**, *4*, 1923.
[16] a)D. L. Ludwig, M. A. MacInnes, Y. Takiguchi, P. E. Purtymun, M. Henrie, M. Flannery, J. Meneses, R. A. Pedersen, D. J. Chen, *Mutat Res* **1998**, *409*, 17; b)S. Xanthoudakis, R. J. Smeyne, J. D. Wallace, T. Curran, *Proc Natl Acad Sci U S A* **1996**, *93*, 8919.
[17] L. B. Meira, S. Devaraj, G. E. Kisby, D. K. Burns, R. L. Daniel, R. E. Hammer, S. Grundy, I. Jialal, E. C. Friedberg, *Cancer Res* **2001**, *61*, 5552.
[18] J. P. Belzile, S. A. Choudhury, D. Cournoyer, T. Y. Chow, *Curr Gene Ther* **2006**, *6*, 111.
[19] A. M. Reed, M. L. Fishel, M. R. Kelley, *Future Oncol* **2009**, *5*, 713.
[20] a)M. L. Fishel, Y. He, M. L. Smith, M. R. Kelley, *Clin Cancer Res* **2007**, *13*, 260; b)M. L. Fishel, M. R. Kelley, *Mol Aspects Med* **2007**, *28*, 375.
[21] M. Luo, M. R. Kelley, *Anticancer Res* **2004**, *24*, 2127.
[22] P. Taverna, L. Liu, H. S. Hwang, A. J. Hanson, T. J. Kinsella, S. L. Gerson, *Mutat Res* **2001**, *485*, 269.
[23] S. Madhusudan, F. Smart, P. Shrimpton, J. L. Parsons, L. Gardiner, S. Houlbrook, D. C. Talbot, T. Hammonds, P. A. Freemont, M. J. Sternberg, G. L. Dianov, I. D. Hickson, *Nucleic Acids Res* **2005**, *33*, 4711.
[24] J. D. Del Rowe, J. Bello, R. Mitnick, B. Sood, C. Filippi, J. Moran, K. Freeman, F. Mendez, R. Bases, *Int J Radiat Oncol Biol Phys* **1999**, *43*, 89.

[25] A. Bapat, M. L. Fishel, M. R. Kelley, *Antioxid Redox Signal* **2009**, *11*, 651.
[26] a)J. E. Guikema, E. K. Linehan, D. Tsuchimoto, Y. Nakabeppu, P. R. Strauss, J. Stavnezer, C. E. Schrader, *J Exp Med* **2007**, *204*, 3017; b)T. T. Koll, S. S. Feis, M. H. Wright, M. M. Teniola, M. M. Richardson, A. I. Robles, J. Bradsher, J. Capala, L. Varticovski, *Mol Cancer Ther* **2008**, *7*, 1985.
[27] A. Bapat, L. S. Glass, M. Luo, M. L. Fishel, E. C. Long, M. M. Georgiadis, M. R. Kelley, *J Pharmacol Exp Ther* **2010**, *334*, 988.
[28] L. A. Seiple, J. H. Cardellina, 2nd, R. Akee, J. T. Stivers, *Mol Pharmacol* **2008**, *73*, 669.
[29] Z. Zawahir, R. Dayam, J. Deng, C. Pereira, N. Neamati, *J Med Chem* **2009**, *52*, 20.
[30] A. Simeonov, A. Kulkarni, D. Dorjsuren, A. Jadhav, M. Shen, D. R. McNeill, C. P. Austin, D. M. Wilson, 3rd, *PLoS One* **2009**, *4*, e5740.
[31] F. A. De Wolff, *BMJ* **1995**, *310*, 1216.
[32] R. Gil-Redondo, J. Estrada, A. Morreale, F. Herranz, J. Sancho, A. R. Ortiz, *J Comput Aided Mol Des* **2009**, *23*, 171.
[33] F. M. Ruiz, R. Gil-Redondo, A. Morreale, A. R. Ortiz, C. Fabrega, J. Bravo, *J Chem Inf Model* **2008**, *48*, 844.
[34] J. Scheper, M. Guerra-Rebollo, G. Sanclimens, A. Moure, I. Masip, D. Gonzalez-Ruiz, N. Rubio, B. Crosas, O. Meca-Cortes, N. Loukili, V. Plans, A. Morreale, J. Blanco, A. R. Ortiz, A. Messeguer, T. M. Thomson, *PLoS One* **2010**, *5*, e11403.
[35] I. D. Kuntz, J. M. Blaney, S. J. Oatley, R. Langridge, T. E. Ferrin, *J Mol Biol* **1982**, *161*, 269.
[36] C. Perez, A. R. Ortiz, *J Med Chem* **2001**, *44*, 3768.
[37] W. Still, A. Tempczyk, R. Hawley, T. hendrickson, *J Am Chem Soc* **1990**, *112*, 6127.
[38] J. J. Irwin, B. K. Shoichet, *J Chem Inf Model* **2005**, *45*, 177.
[39] D. M. Wilson, 3rd, D. Barsky, *Mutat Res* **2001**, *485*, 283.
[40] a)W. C. Tse, D. L. Boger, *Curr Protoc Nucleic Acid Chem* **2005**, *Chapter 8*, Unit 8 5; b)D. L. Boger, B. E. Fink, S. R. Brunette, W. C. Tse, M. P. Hedrick, *J Am Chem Soc* **2001**, *123*, 5878.
[41] a)J. A. Loo, *Mass Spectrom Rev* **1997**, *16*, 1; b)B. N. Pramanik, P. L. Bartner, U. A. Mirza, Y. H. Liu, A. K. Ganguly, *J Mass Spectrom* **1998**, *33*, 911.
[42] a)M. Karas, U. Bahr, T. Dulcks, *Fresenius J Anal Chem* **2000**, *366*, 669; b)M. Wilm, M. Mann, *Anal Chem* **1996**, *68*, 1.
[43] J. L. Benesch, C. V. Robinson, *Curr Opin Struct Biol* **2006**, *16*, 245.
[44] D. R. McNeill, D. M. Wilson, 3rd, *Mol Cancer Res* **2007**, *5*, 61.
[45] M. D. Wyatt, D. L. Pittman, *Chem Res Toxicol* **2006**, *19*, 1580.
[46] R. Eritja, P. A. Walker, S. K. Randall, M. F. Goodman, B. E. Kaplan, *Nucleosides Nucleotides* **1987**, *6*, 11.
[47] P. T. Beernink, B. W. Segelke, M. Z. Hadi, J. P. Erzberger, D. M. Wilson, 3rd, B. Rupp, *J Mol Biol* **2001**, *307*, 1023.
[48] G. Barzilay, C. D. Mol, C. N. Robson, L. J. Walker, R. P. Cunningham, J. A. Tainer, I. D. Hickson, *Nat Struct Biol* **1995**, *2*, 561.
[49] W. D. Cornell, P. Cieplak, B. C. I., G. I. R., K. M. Merz, D. M. Ferguson, D. C. Spellmeyer, T. Fox, C. J. W., P. A. Kollman, *J Am Chem Soc* **1995**, *117*, 5179.
[50] Gordon, **2005**.
[51] D. F. Lowry, D. W. Hoyt, F. A. Khazi, J. Bagu, A. G. Lindsey, D. M. Wilson, 3rd, *J Mol Biol* **2003**, *329*, 311.
[52] C. D. Mol, T. Izumi, S. Mitra, J. A. Tainer, *Nature* **2000**, *403*, 451.
[53] P. A. Kollman, I. Massova, C. Reyes, B. Kuhn, S. Huo, L. Chong, M. Lee, T. Lee, Y. Duan, W. Wang, O. Donini, P. Cieplak, J. Srinivasan, D. A. Case, T. E. Cheatham, 3rd, *Acc Chem Res* **2000**, *33*, 889.
[54] D. Weininger, *J Chem Inf Comput Sci* **1988**, *28*, 31.
[55] C. M. Networks., *E., Germany* **2000**.
[56] J. J. Stewart, *J Comput Aided Mol Des* **1990**, *4*, 1.
[57] R. Gil Redondo, *UNED* **2006**.
[58] A. Morreale, R. Gil-Redondo, A. R. Ortiz, *Proteins* **2007**, *67*, 606.
[59] J. Ryckaert, G. Ciccotti, H. Berendsen, *J Comp Phys* **1977**, *23*, 327.
[60] T. Darden, D. York, L. Pedersen, *J Chem Phys* **1993**, *98*, 10089.
[61] W. Jorgensen, J. Chandrasekhar, J. Madura, R. Impey, M. Klein, *J Chem Phys* **1983**, *79*, 926.
[62] S. L. McGovern, E. Caselli, N. Grigorieff, B. K. Shoichet, *J Med Chem* **2002**, *45*, 1712.
[63] W. L. DeLano, *DeLano Scientific, Palo Alto, CA, USA* **2002**.

GRAFICAL ABSTRACT

Rational design. *Here we report the identification by docking-based virtual screening of six compounds as potential Ape1 inhibitors. These compounds showed inhibitory activity in vitro in the low-medium μM range and they also potentiated the cytotoxicity of MMS in fibrosarcoma cells. This study opens the door to the development of a new generation of Ape1 inhibitors.*